



Charged particle periodicities in Saturn's outer magnetosphere

J. F. Carbary,¹ D. G. Mitchell,¹ S. M. Krimigis,¹ D. C. Hamilton,² and N. Krupp³

Received 16 February 2007; revised 30 March 2007; accepted 10 April 2007; published 29 June 2007.

[1] A Lomb periodogram analysis is applied to charged particle data from the LEMMS/CHEMS instruments on the Cassini spacecraft. The data represent count rates, averaged within 30 min bins, from electrons (28–330 keV) and protons and oxygen ions (2.8–236 keV) during 350 days in 2005 and all 365 days in 2006. Sun effects, spacecraft maneuvers, and measurements within 20 R_S of Saturn were removed from the data prior to analysis. The main peaks in the frequency periodograms (or power spectra) were found within a frequency window from 9.5 hours to 12.5 hours. For signal-to-noise ratios exceeding 8, the periodograms within this window reveal a consistent peak near 10.80 hours (10 hours 48 min 36 sec) for all the charged particles regardless of energy or species. Even for lower signal-to-noise ratios, a peak near this period is generally present. The Lomb analyses are consistent with an azimuthal anomaly that rotates with a period of 10.80 hours.

Citation: Carbary, J. F., D. G. Mitchell, S. M. Krimigis, D. C. Hamilton, and N. Krupp (2007), Charged particle periodicities in Saturn's outer magnetosphere, *J. Geophys. Res.*, 112, A06246, doi:10.1029/2007JA012351.

1. Introduction

[2] The planet Saturn displays a variety of periodicities thought to be associated with its rotation. Spin-periodicities include those of the planetary radio emissions [Desch and Kaiser, 1981; Gurnett *et al.*, 2005], the magnetic field [Espinosa and Dougherty, 2000; Espinosa *et al.*, 2003; Giampieri *et al.*, 2006], magnetospheric charged particles and their spectra [Carbary and Krimigis, 1982; Krupp *et al.*, 2005; Carbary *et al.*, 2007], energetic neutral particles [Krimigis *et al.*, 2005; Paranicas *et al.*, 2005], total electron density in Saturn's inner magnetosphere [Gurnett *et al.*, 2007], and even spokes in Saturn's ring system [Porco and Danielson, 1982]. The kilometric radio variations (SKR) have been used to define a longitude system [Davies *et al.*, 1996]. However, Saturn's radio period was later found to change slowly [Galopeau and Lecacheux, 2000; Gurnett *et al.*, 2005], and the systematics of this drift can be used to define a dynamic longitude system [Kurth *et al.*, 2007].

[3] Previous studies of charged particle periodicities at Saturn have heretofore involved limited data sets of a few days at most [e.g., Krupp *et al.*, 2005; Carbary *et al.*, 2007]. While useful, such an approach may miss important consequences of a larger-scale study and does not confer the authority of a statistical analysis. The current study performs just such a large-scale, statistical analysis. A Lomb periodogram analysis is applied to two years of charged particle data obtained by the Magnetospheric Imaging

Instrument (MIMI) on the Cassini spacecraft. The investigation also extends the previous studies by including protons and oxygen ions as well as electrons.

2. Data Set

[4] All data used herein derive from observations made by the MIMI instrument on the Cassini spacecraft. Krimigis *et al.* [2004] fully describe this instrument, which consists of the Ion and Neutral Camera (INCA), the Low Energy Magnetospheric Measurement System (LEMMS), and the Charge Energy Mass Spectrometer (CHEMS). This investigation uses electron data from the LEMMS sensor, and proton (H^+) and oxygen ion (O^+) data from the CHEMS instrument. The electron data used here were accumulated in five logarithmically spaced energy channels from 28 keV to 330 keV. The proton and oxygen ion data come from four CHEMS energy bins from 3 to 236 keV.

[5] The raw data consist of counts per second in each of the channels at a time resolution of several seconds. The electron data may contain spurious counts from Sun-contamination, maneuvers, etc., and these were removed at this time resolution before further processing. To improve statistics, the count rates were averaged into half-hour time bins for the three species of charged particles. The averaging was conducted for all available data from 2005 and 2006. After averaging, the signals are conditioned with a 48-point detrending kernel followed by a seven-point smoothing, both of which use the SMOOTH procedure in the Interactive Data Language (IDL) library.

[6] Figure 1 illustrates the totality of these data in an orbital format, with each point representing a single half-hour average. Data from 2005 come primarily from the dawn and postdawn sector at generally southern latitudes, while data from 2006 come primarily from the midnight and predawn sector at near-equatorial latitudes. Because Saturn

¹Johns Hopkins University Applied Physics Laboratory, Laurel, Maryland, USA.

²Department of Physics, University of Maryland, College Park, Maryland, USA.

³Max-Planck-Institut für Sonnensystemforschung, Lindau, Germany.

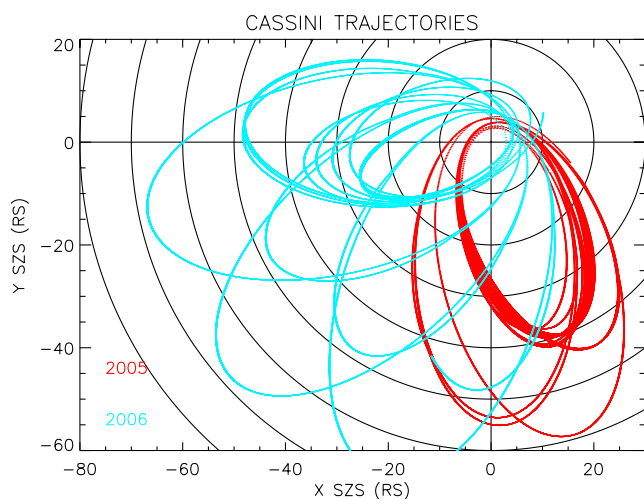


Figure 1. Totality of the charged particle data from 2005 and 2006 used in this investigation. The view is from the north pole of Saturn with the Sun along the X axis to the right. Red trajectories are from 2005, and the blue trajectories are from 2006.

periodicities might have a local time and/or latitude dependence, results from the two years were segregated. Furthermore, only data outside $20 R_S$ are used. Inside $20 R_S$, satellite absorption or emission may affect charged particle periodicities. Furthermore, the speed of the satellite within $\sim 20 R_S$ may introduce Doppler effects on the periodicities

[e.g., Cowley *et al.*, 2006]; outside $20 R_S$, the satellite moves more slowly and, because expected magnetospheric motions are rapid, Doppler effects are much less [e.g., Carbary *et al.*, 2007]. Simulations (discussed below) also indicate Doppler effects can be ignored outside $20 R_S$ and probably at even smaller radial distance.

[7] Figure 2 shows all of the unfiltered proton data for 2006 (top) as well as 5 days of data in detail (bottom). The quasi-regular oscillations in the top panel represent the close encounters of the satellite with Saturn's inner magnetosphere and result purely from the orbital motion of Cassini. These oscillations have nothing to do with Saturn's periodicities, of course, and are removed by low-frequency filtering. Figure 2 (bottom) shows an expanded view of the regular oscillations that are almost always observed in Saturn's outer magnetosphere. These oscillations have a period of approximately 11 hours. The objective of this investigation is the statistical determination of these oscillations.

3. Analysis

[8] Subject to the constraints and filters discussed in the previous section, half-hour averages of electron, proton, and oxygen ion count rates were subjected to a Lomb periodogram analysis. A Lomb periodogram analysis is similar to a Fourier analysis in that both transform a signal in the time domain to the frequency domain to produce a power spectrum. However, a Lomb analysis has significant advantages over a Fourier analysis. A Lomb analysis does not require equally-spaced data points in time and can successfully operate in the presence of data gaps, even if they are a

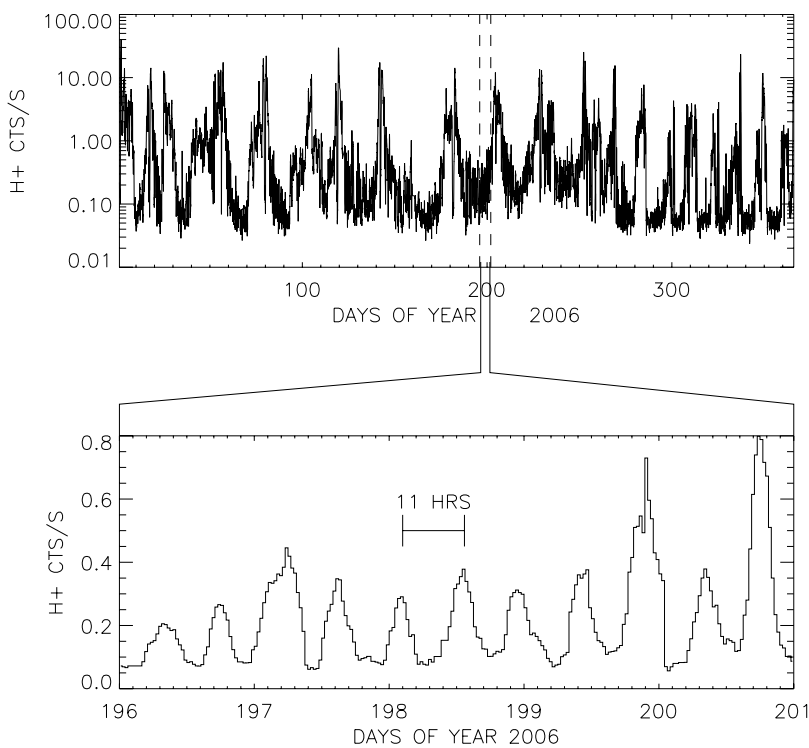


Figure 2. Proton (2.8–7.7 keV) count rate profile (top) for all of 2006 and (bottom) detailed count rate profile for 5 days. During the selected interval, the spacecraft was traveling inbound from $\sim 45 R_S$ to $\sim 30 R_S$ in the postmidnight sector of Saturn's magnetotail. Periodic variations near the 10.76 hour SKR period are apparent.

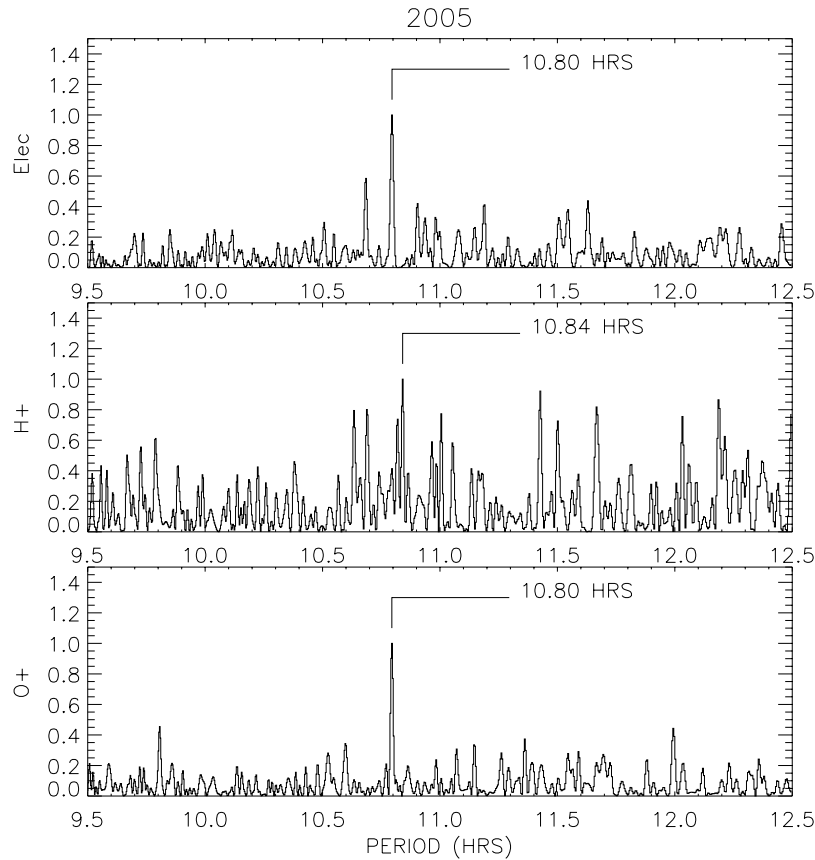


Figure 3. Lomb spectra for (top) 20–33 keV electrons, (middle) 2.8–8.3 keV protons, and (bottom) 8.3–26 keV oxygens for all available days in 2005. The data have been subjected to the filters and constraints discussed in the text. The periods of the main spectral peaks are indicated; the power spectra have been normalized to the maximum.

significant portion of the entire sampling interval. A Lomb analysis can also overcome rather severe noise in a signal and still provide a robust estimate of the periodicity. The significance number that is output from a Lomb analysis provides an estimate of the significance of any peaks in the power spectrum. The analysis here uses the LNP_TEST procedure in the IDL library, which is based on a discussion given by *Press et al.* [1992].

[9] Lomb periodograms were constructed for the separate years of 2005 and 2006. Peaks were found in the spectral region between 9.5 hours and 12.5 hours ($f = 0.105$ and 0.080 hr^{-1} , respectively, where f is frequency). This spectral filtering removed any low-frequency peaks associated with orbits of the spacecraft as well as any higher-frequency peaks that are here considered irrelevant to the rotational modulation of Saturn. For each charged particle species, one dominant peak generally appeared within this spectral region. One measure of the uncertainty of the peak is its full width at half maximum (FWHM). For all peaks, the FWHM translates to an error in the period of less than 0.01 hours, meaning the peaks are very narrow. Another measure of the certainty of the periodicity is the Lomb significance number, which lies in the interval between 0 and 1. The significance numbers were all less than $\sim 1 \times 10^{-6}$, and usually much less. (A number close to 0 indicates high confidence of a periodicity, while a number close to 1 indicates low confidence.) A more familiar indicator of

confidence is signal-to-noise ratio (SNR), which is defined here as the ratio of the peak power to the standard deviation of the power within the spectral window of interest. A discussion of SNR is beyond the scope of this paper, but an SNR of ~ 6 is usually considered sufficient to detect a “target” against a “cluttered” background [e.g., *Jamieson, 1978*]. SNRs derived here are generally of this magnitude or larger.

4. Results

[10] Figure 3 displays sample Lomb periodograms for 2005, and Figure 4 shows the same for 2006. In each case, only the spectral range from 9.5 hours to 12.5 hours is shown, and the power has been normalized to the maximum within this frequency band. Periodograms for electrons, protons and oxygen ions are compared in each figure.

[11] For both 2005 and 2006, prominent peaks appear at or near the optimized 10.793 hour SKR period [*Kurth et al., 2007*]. For 2005, the electron and oxygen ion periodic signals are particularly strong (SNR = 10.6 and 11.6, respectively), while the proton signal is among the weakest in the Lomb results (SNR = 5.2). For 2006, the electron period is again very strong (SNR = 12.8), while the proton signal is stronger than the oxygen ion signal (SNR = 11.7 versus SNR = 7.7). When the SNR is sufficiently large, generally exceeding ~ 8 , the Lomb peak periods tend to have a

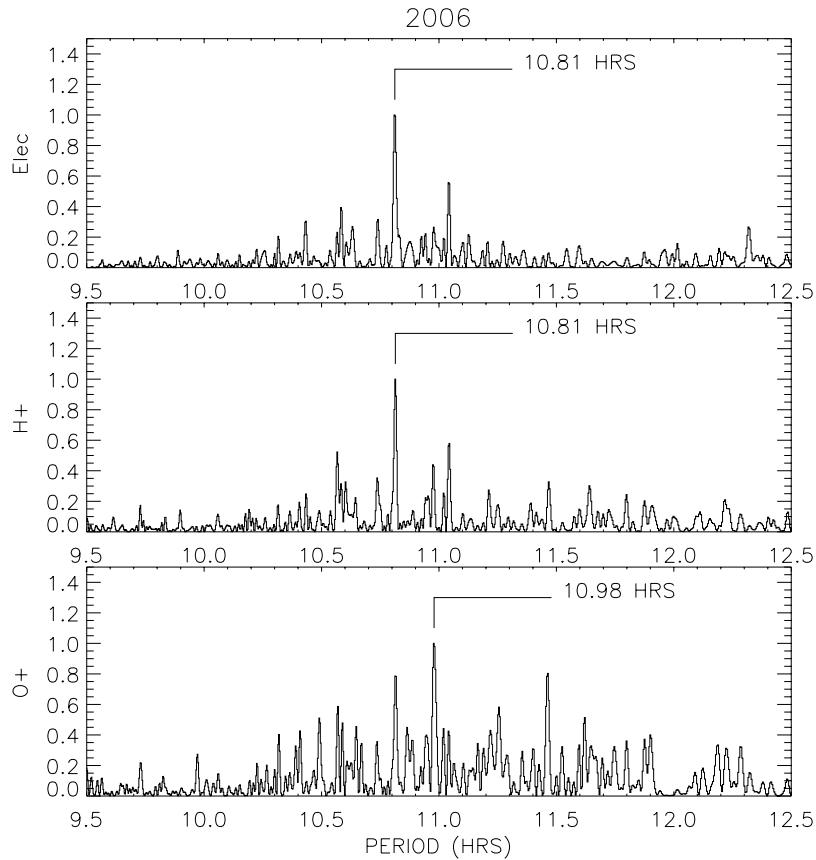


Figure 4. Lomb spectra for (top) 20–33 keV electrons, (middle) 2.8–8.3 keV protons, and (bottom) 8.3–26 keV oxygens for all available days in 2006 in the same format as Figure 3.

value of 10.80 hours, which is very close to the 10.793 hour SKR period. Even in cases when the SNR is marginal, however, a secondary peak appears in the Lomb periodogram very close to 10.80 hours (e.g., Figure 4, bottom).

[12] Figure 5 shows the Lomb periods as a function of signal to noise ratio and compares them to IAU, SKR, and magnetic field periods. Two salient features emerge from

this figure: the charged particle periods converge for SNRs exceeding about 8, and the convergence value is essentially the same (10.8 hours) as that observed in the kilometric radiation and the magnetic fields [Kurth *et al.*, 2007; Giampieri *et al.*, 2006]. Peculiarly, the low SNR periods are all longer than the 10.8 hours, although the reason for this is not known.

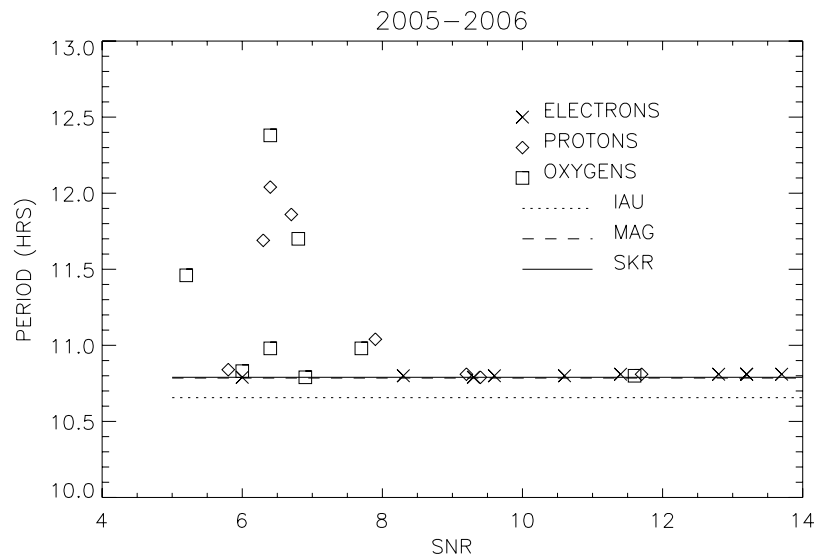


Figure 5. Lomb periods (from peaks in Lomb periodograms for 9.5 to 12.5 hours) as a function of signal to noise ratio (SNR). The IAU, SKR, and magnetometer periodicities are shown for comparison.

Table 1. Periods and Signal to Noise Ratios for Lomb Analyses

Species	2005		2006	
	Period, hours	SNR	Period, hours	SNR
e ⁻ (28.–49. keV)	10.80	10.6	10.81	12.8
e ⁻ (41.–64. keV)	10.80	9.6	10.81	13.2
e ⁻ (58.–102. keV)	10.80	8.3	10.81	13.2
e ⁻ (96.–196. keV)	10.79	6.0	10.81	11.4
e ⁻ (187.–330. keV)	10.79	9.3	10.81	13.7
H ⁺ (3.–8. keV)	10.84	5.8	10.81	11.7
H ⁺ (8.–26. keV)	12.04	6.4	10.81	9.2
H ⁺ (27.–78. keV)	11.69	6.3	11.04	7.9
H ⁺ (82.–236. keV)	10.79	9.4	11.86	6.7
O ⁺ (3.–8. keV)	10.83	6.0	11.46	5.2
O ⁺ (8.–26. keV)	10.80	11.6	10.98	7.7
O ⁺ (27.–78. keV)	11.70	6.8	10.98	6.4
O ⁺ (82.–236. keV)	10.79	6.9	12.38	6.4

[13] Table 1 gives the same results plotted in Figure 5. Particle species and energies are given in the left-hand column. Their Lomb peak periods and SNRs for 2005 are in the next two columns, and the last two columns give the Lomb periods and SNRs for 2006. The periods for all species are consistently 10.80 hours for both years when the SNR is sufficiently large (i.e., when it is greater than 8). Even when the SNR is smaller than 8, some periods are close to the 10.8 hour period.

5. Discussion

[14] The Lomb analysis has several minor limitations worth mentioning. First, the data samples come from a restricted region of the magnetosphere, namely, the dawn and midnight sectors. Undoubtedly, some of the measurements were also taken outside the magnetopause where Saturn periodicity is not probable (although Jovian perio-

dicities are observed outside of Jupiter’s magnetosphere, so a rotation-related periodicity outside Saturn’s magnetopause is plausible). Whether charged particles display consistent periodicities in other local time sectors has yet to be determined. Second, the spectra discussed here are restricted to frequency ranges of 9.5 hours to 12.5 hours, which brackets the periodicities one might reasonably expect for Saturn. One might expect a peak at the much longer period associated with the orbital period of Cassini ($\gg 12.5$ hours). One might also expect a peak at a shorter period of ~ 5 hours associated with double crossings of a (possibly) wavy current sheet in Saturn’s magnetotail (although Lomb spectra near $f = 1/5 \text{ hr}^{-1}$, not shown here, are unremarkable.) Finally, some of the data used here do suffer from low count rates, especially in the higher energy ion channels. This problem can be overcome to a large extent by the half-hour averages used here. Nevertheless, much of the low signal to noise ratios evident in the higher energy channels is caused by poor statistics. That a Lomb analysis can delineate a peak from such noisy data testifies to the method’s robustness.

[15] Perhaps the simplest way to interpret the 10.80-hour periodicity involves a density enhancement or “anomaly” that rotates with the planet. The anomaly can produce a cam-like effect that launches density waves from the inner magnetosphere [e.g., *Espinosa et al.*, 2003; *Cowley et al.*, 2006], and the outgoing waves would have a 10.80-hour periodicity. A rigidly corotating anomaly would also produce such an effect [e.g., *Carbary et al.*, 2007]. The count rates $C(r, z, t)$ from such an anomaly might be heuristically modeled by, for example,

$$C(r, z, t) = C_0 \exp[-r/r_0] \exp\left[-(z/z_0)^2\right] [1 + \cos(\omega t - \phi(t))] \quad (1)$$

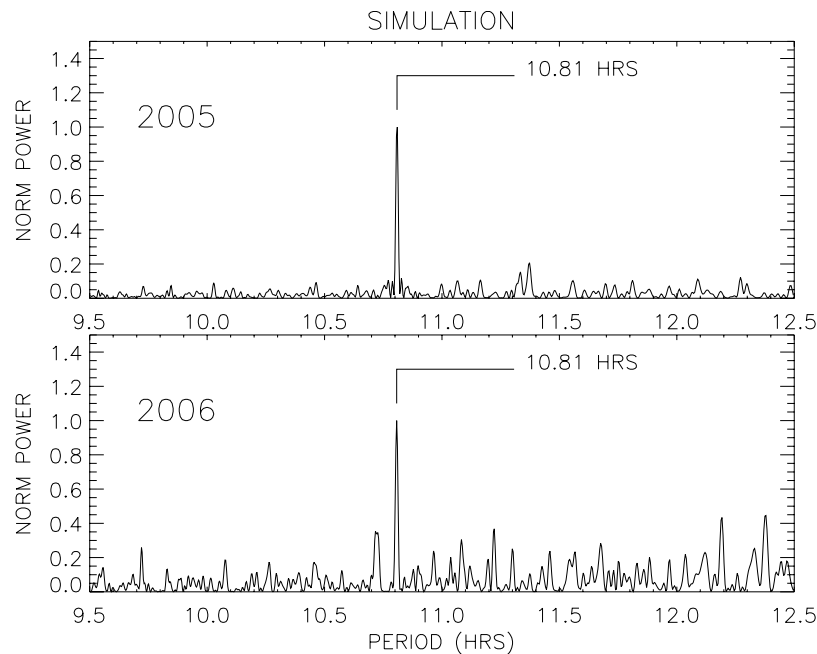


Figure 6. Simulated Lomb spectra expected from an anomaly rotating with a period of 10.81 hours. The simulated count rate signal had random noise of up to 200% of the signal added and 50 random gaps ranging in size from 0.5 to 5.0 hours; as with the observed spectra, only data from outside $20 R_S$ were used. The spectra are normalized to their maxima.

where $r_0 = 20 R_S$ is an e-folding distance in radius, $z_0 = 5 R_S$ is the half-thickness of a current sheet, $\omega = 2\pi/T$ is the angular frequency for a corotation period of T ($= 10.81$ hours here), and $\phi(t)$ is the phase (local time) of the spacecraft. C_0 is a constant, which can be ignored because only the relative variations are sought. Cylindrical coordinates are used. A Doppler shift may be included in (1) by adjusting the angular frequency:

$$\omega = (2\pi/T) \cdot [1 - (v/w) \cdot \cos \alpha] \quad (2)$$

where v is the spacecraft velocity, w is the wave velocity, and α is the angle between them. The model developed here assumed negligible Doppler shift in which $(v/w) \cdot \cos \alpha \ll 1$.

[16] An entire year can be simulated by inserting the Cassini orbits in (1). To make the simulation more realistic, random noise and gaps are added and count rates within $20 R_S$ are removed. Figure 6 displays the Lomb periodograms resulting from simulations for Cassini trajectories in 2005 and 2006. The 10.81-hour period is clearly apparent in both simulations. The 2005 SNR is 16.9, and the 2006 SNR is 11.4. Both simulations exhibit noise resulting from an obfuscated signal, but the Lomb periodogram clearly extracts the principal period.

6. Conclusions

[17] A Lomb periodogram analysis of 2 years' worth of charged particle data indicates that Saturn's outer magnetosphere has periodicity of about 10.80 hours. Electron, proton, and oxygen ion periodicities are consistent as long as the SNR of their Lomb periodogram exceeds 8. The periodicities are the same for all charged particles. Periodicities are the same in dawn and midnight sectors, and apparently at southern latitudes and equatorial latitudes, and the periods are consistent with magnetometer and Saturn kilometric radiation periods. The accuracy of the Lomb method is not (yet) sufficient to determine if the charged particle period has drifted over the 2 year period sampled here. The results are consistent with a "noisy" azimuthal anomaly that rotates with period of 10.80 hours.

[18] **Acknowledgments.** We would like to thank our colleagues Pontus Brandt, Chris Paranicas, and Ed Roelof at the Applied Physics Laboratory, Johns Hopkins University, for helpful discussions about Saturn's magnetosphere, and Jon Vandegriff for assistance with data processing. This research was supported by the NASA Office of Space Science under Task Order 003 of contract NAS5-97271 between NASA Goddard Space Flight Center and the Johns Hopkins University.

[19] Wolfgang Baumjohann thanks Donald Gurnett and another reviewer for their assistance in evaluating this paper.

References

- Carbary, J. F., and S. M. Krimigis (1982), Charged particle periodicity in the Saturnian magnetosphere, *Geophys. Res. Lett.*, *9*, 1073–1076.
- Carbary, J. F., D. G. Mitchell, S. M. Krimigis, and N. Krupp (2007), Electron periodicities in Saturn's outer magnetosphere, *J. Geophys. Res.*, *112*, A03206, doi:10.1029/2006JA012077.
- Cowley, S. W. H., et al. (2006), Cassini observations of planetary-period magnetic field oscillations in Saturn's magnetosphere: Doppler shifts and phase motion, *Geophys. Res. Lett.*, *33*, L07104, doi:10.1029/2005GL025522.
- Davies, M. E., et al. (1996), Report for the IAU/IAG/COSPAR working group on cartographic coordinates and rotational elements of the planets and satellites: 1994, *Celest. Mech. Dyn. Astron.*, *63*, 127–148.
- Desch, M. D., and M. L. Kaiser (1981), Voyager measurement of the rotation period of Saturn's magnetic field, *Geophys. Res. Lett.*, *8*, 253–256.
- Espinosa, S. A., and M. K. Dougherty (2000), Periodic perturbations in Saturn's magnetic field, *Geophys. Res. Lett.*, *27*, 2785–2788.
- Espinosa, S. A., D. J. Southwood, and M. K. Dougherty (2003), Reanalysis of Saturn's magnetospheric field data view of spin-periodic perturbations, *J. Geophys. Res.*, *108*(A2), 1085, doi:10.1029/2001JA005083.
- Galopeau, P. H. M., and A. Lecacheux (2000), Variations of Saturn's radio period measured at kilometer wavelengths, *J. Geophys. Res.*, *105*, 13,089–13,101.
- Giampieri, G., M. K. Dougherty, E. J. Smith, and C. T. Russell (2006), A regular period for Saturn's magnetic field that may track its internal rotation, *Nature*, *441*, 62–64, doi:10.1038/nature04750.
- Gurnett, D. A., et al. (2005), Radio and plasma wave observations at Saturn from Cassini's approach and first orbit, *Science*, *307*, 1255–1259, doi:10.1126/science.1105356.
- Gurnett, D. A., A. M. Persoon, W. S. Kurth, J. B. Groene, T. F. Averkamp, M. K. Dougherty, and D. J. Southwood (2007), The variable rotation period of the inner region of Saturn's plasma disk, *ScienceExpress*, doi:10.1126/science.1138562.
- Jamieson, J. J. (1978), Warning systems, in *The Infrared Handbook*, edited by W. W. Wolfe and G. J. Zeiss, pp. 21-1–21-33, U.S. Govt. Print. Off., Washington, D. C.
- Krimigis, S. M., et al. (2004), Magnetosphere Imaging Instrument (MIMI) on the Cassini Mission to Saturn, *Space Sci. Rev.*, *114*, 233–329.
- Krimigis, S. M., et al. (2005), Dynamics of Saturn's magnetosphere from MIMI during Cassini's orbital insertion, *Science*, *307*, 1270–1273.
- Krupp, N., et al. (2005), The Saturnian plasma sheet as revealed by energetic particle measurements, *Geophys. Res. Lett.*, *32*, L20S03, doi:10.1029/2005GL022829.
- Kurth, W. S., A. Lecacheux, T. F. Averkamp, J. B. Groene, and D. A. Gurnett (2007), A Saturnian longitude system based on a variable kilometric radiation period, *Geophys. Res. Lett.*, *34*, L02201, doi:10.1029/2006GL028336.
- Paranicas, C., D. G. Mitchell, E. C. Roelof, P. C. Brandt, D. J. Williams, S. M. Krimigis, and B. H. Mauk (2005), Periodic intensity variations in global ENA images of Saturn, *Geophys. Res. Lett.*, *32*, L21101, doi:10.1029/2005GL023656.
- Porco, C. C., and G. E. Danielson (1982), The periodic variation of spokes in Saturn's rings, *Astron. J.*, *87*, 826–829.
- Press, W. H., S. A. Teukolsky, W. T. Vetterling, and B. P. Flannery (1992), *Numerical Recipes: The Art of Scientific Computing*, pp. 569–577, Cambridge Univ. Press, Cambridge, U. K.
- J. F. Carbary, S. M. Krimigis, and D. G. Mitchell, Johns Hopkins University Applied Physics Laboratory, Laurel, MD 20713, USA. (james.carbary@jhuapl.edu)
- D. C. Hamilton, Department of Physics, University of Maryland, College Park, MD 20742, USA.
- N. Krupp, Max-Planck-Institut für Sonnensystemforschung, D-37191, Lindau, Germany.